Article

Cell Reports

ARHGAP12 Functions as a Developmental Brake on Excitatory Synapse Function

Graphical Abstract

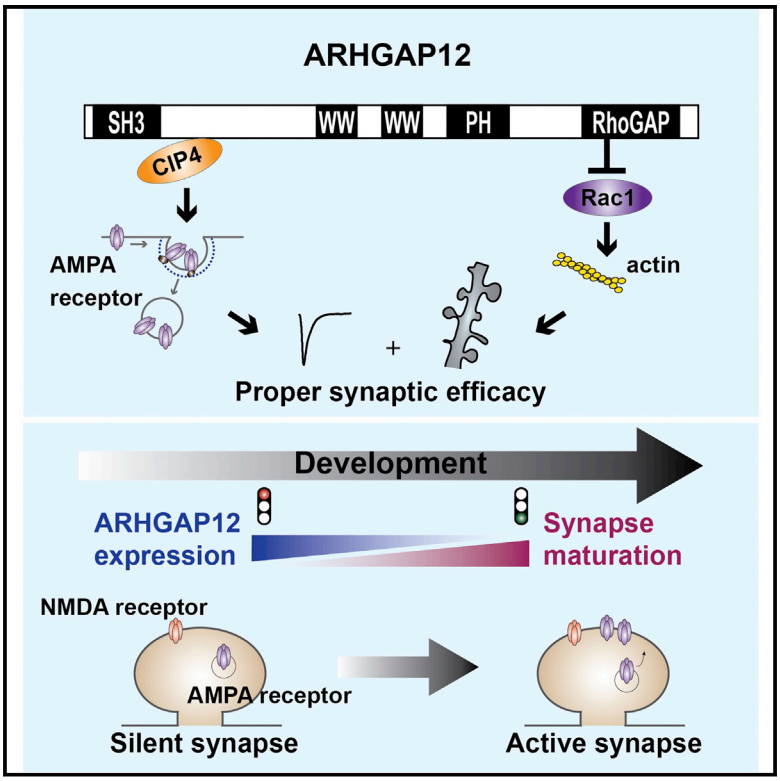

Authors

W. Ba, M.M. Selten, J. van der Raadt, ..., M.J. Courtney, H. van Bokhoven, N. Nadif Kasri

Correspondence

n.nadif@donders.ru.nl

In Brief

Ba et al. find that the Rac1 GAP, ARHGAP12, coordinates dendritic spine morphology and synaptic strength via its GAP activity and interaction with CIP4, respectively. ARHGAP12 limits synapse maturation by restricting silent synapses converting to functional synapses in the developing hippocampus.

Highlights

- ARHGAP12 functions at excitatory synapses of CA1 hippocampal neurons
- ARHGAP12 promotes postsynaptic AMPA receptor endocytosis
- ARHGAP12 restricts synaptic maturation by limiting silent synapse unsilencing

Ba et al., 2016, Cell Reports *14*, 1355–1368
February 16, 2016
http://dx.doi.org/10.1016/j.celrep.2016.01.037

Cell Reports
Article

ARHGAP12 Functions as a Developmental Brake on Excitatory Synapse Function

W. Ba,[1,2,3] M.M. Selten,[1,2,3] J. van der Raadt,[2,4] H. van Veen,[3,8] L.-L. Li,[5] M. Benevento,[1,2,3] A.R. Oudakker,[1,2,3] R.S.E. Lasabuda,[2] S.J. Letteboer,[2,4] R. Roepman,[2,4] R.J.A. van Wezel,[3,7] M.J. Courtney,[5,6] H. van Bokhoven,[1,2,3,4] and N. Nadif Kasri[1,2,3,*]

[1]Department of Cognitive Neuroscience, Radboudumc, 6500 HB Nijmegen, the Netherlands
[2]Department of Human Genetics, Radboudumc, 6500 HB Nijmegen, the Netherlands
[3]Donders Institute for Brain, Cognition, and Behaviour, 6525 AJ Nijmegen, the Netherlands
[4]Radboud Institute for Molecular Life Sciences, Radboudumc, 6525 GA Nijmegen, the Netherlands
[5]Molecular Signalling Laboratory, Department of Neurobiology, A.I. Virtanen Institute, University of Eastern Finland, Kuopio 70210, Finland
[6]Turku Centre for Biotechnology, Abo Akademi University and University of Turku, Turku 20521, Finland
[7]Biomedical Signal and Systems, MIRA Institute for Biomedical Technology and Technical Medicine, University of Twente, 7500 AE Enschede, the Netherlands
[8]Division of Pharmacology, Utrecht Institute for Pharmaceutical Sciences, Faculty of Science, Utrecht University, P.O. Box 80082, 30508 TB Utrecht, the Netherlands
*Correspondence: n.nadif@donders.ru.nl
http://dx.doi.org/10.1016/j.celrep.2016.01.037

SUMMARY

The molecular mechanisms that promote excitatory synapse development have been extensively studied. However, the molecular events preventing precocious excitatory synapse development so that synapses form at the correct time and place are less well understood. Here, we report the functional characterization of ARHGAP12, a previously uncharacterized Rho GTPase-activating protein (RhoGAP) in the brain. ARHGAP12 is specifically expressed in the CA1 region of the hippocampus, where it localizes to the postsynaptic compartment of excitatory synapses. ARHGAP12 negatively controls spine size via its RhoGAP activity and promotes, by interacting with CIP4, postsynaptic AMPA receptor endocytosis. *Arhgap12* knockdown results in precocious maturation of excitatory synapses, as indicated by a reduction in the proportion of silent synapses. Collectively, our data show that ARHGAP12 is a synaptic RhoGAP that regulates excitatory synaptic structure and function during development.

INTRODUCTION

The dynamic process of formation and fine-tuning of synaptic connections between neurons is critical for neuronal development and proper brain function (Li and Sheng, 2003; McAllister, 2007). Most excitatory synapses are located on dendritic spines, small filamentous actin (F-actin)-enriched protrusions on dendrites (Hotulainen and Hoogenraad, 2010). Synaptic efficiency is rapidly modified during development or in response to changes in activity by remodeling of spine structure and trafficking of glutamate ionotropic alpha-amino-3-hydroxy-5-methyl-4-isoxazole propionic acid receptors (AMPARs; Chater and Goda, 2014).

Several observations have shown that the number of AMPARs and the geometry of dendritic spines are tightly correlated (Engert and Bonhoeffer, 1999; Kopec and Malinow, 2006; Matsuzaki et al., 2004). Actin remodeling, which occurs in dendritic spines, drives changes in spine morphology and is required, but not sufficient, for stable long-term potentiation (LTP), one of the core mechanisms of synaptic plasticity underlying learning and memory (Cingolani and Goda, 2008; Malinow and Malenka, 2002). Inhibition of spine enlargement by blocking actin polymerization prevents proper LTP expression (Fukazawa et al., 2003; Ramachandran and Frey, 2009), whereas increasing spine size alone, by promoting actin polymerization, is not sufficient to express LTP (Cingolani and Goda, 2008; Okamoto et al., 2004; Wang et al., 2007). Evidence suggests that impairments in spine structure and synaptic strength during development contribute to numerous neurological diseases, including intellectual disability (ID), autism spectrum disorder (ASD), and schizophrenia (Nadif Kasri and Van Aelst, 2008; Penzes et al., 2011; Phillips and Pozzo-Miller, 2015; Xu et al., 2014).

How modifications in spine structure and synaptic strength are coordinated, however, remains largely unknown. As key regulators of the actin cytoskeleton, the Rho subfamily members of guanosine triphosphate (GTP)-binding proteins play a critical role in synapse formation, maturation, and maintenance, directly affecting both synapse structure and function (Ba et al., 2013; Nadif Kasri and Van Aelst, 2008; Tolias et al., 2011). Members of the Rho subfamily of GTP-binding proteins act as molecular switches cycling between an active GTP-bound form and an inactive guanosine diphosphate-bound form. Their activity is mainly regulated by guanine nucleotide exchange factors (GEFs), which are positive regulators, and by guanosine

triphosphatase (GTPase)-activating proteins (GAPs) and guanine nucleotide dissociated inhibitors, which are negative regulators (Van Aelst and D'Souza-Schorey, 1997). GEFs and GAPs are typically multi-domain proteins, and their expression levels are tightly regulated during development. Their specific spatial and temporal expression patterns enable them to regulate synaptic function through the interaction with diverse upstream molecules and downstream effectors (Tolias et al., 2011). Several Rho GEFs and GAPs have been shown to uniquely regulate synaptic development and plasticity (Duman et al., 2015; Guerrier et al., 2009; Ip et al., 2012). In addition, a number of Rho GTPase regulators and effectors have been directly associated with ID, including Oligophrenin-1 (Nadif Kasri et al., 2009, 2011), OCRL1 (Hichri et al., 2011), ARHGEF6 (Kutsche et al., 2000), and PAK3 (Allen et al., 1998). However, remarkably little is known about how individual GEFs or GAPs precisely coordinate synaptic morphology and function during development.

In this study, we focused on ARHGAP12, a RhoGAP that negatively regulates Rac1 signaling and whose function has not yet been described in the brain. We found that ARHGAP12 is almost exclusively expressed in hippocampal CA1 neurons during early stages of development. We investigated the postsynaptic function of ARHGAP12 by spatially and temporally manipulating the levels of ARHGAP12, specifically at hippocampal CA3-CA1 synapses. We characterized ARHGAP12 as a structure-function coordinator of excitatory synapses during hippocampal development. Our results uncover a dual function for ARHGAP12 in coordinating synaptic structure and AMPAR trafficking in hippocampal CA3-CA1 synapses during development.

RESULTS

Expression and Distribution of ARHGAP12 in the Hippocampus

To identify Rho GTPase regulators that are critical for the development of cell-type-specific synapses in the hippocampus, we used the mRNA expression data from the Allen Brain Atlas (http://mouse.brain-map.org/). We focused on Rho GTPase regulators with a specific spatial expression pattern. We identified the Rac1 GAP protein, ARHGAP12 (Gentile et al., 2008), as an interesting candidate protein based on its specific CA1 and, to a lesser extent, dentate gyrus (DG) expression (Figure 1A). We initiated the characterization of ARHGAP12 by determining its spatiotemporal distribution in the rat hippocampus. Immunostaining experiments revealed that ARHGAP12 was prominently expressed in the hippocampal CA1 region and to a lesser extent in the DG, confirming the mRNA expression data. ARHGAP12 was detected in all hippocampal CA1 pyramidal cell layers, in the somata, and along the dendrites (Figure 1B). We next examined the expression of ARHGAP12 during different stages of hippocampal development by western blot. ARHGAP12 was abundantly expressed in embryonic day 18 (E18) and early postnatal (1–2 weeks) hippocampus; thereafter, its expression gradually declined into adulthood. In adult hippocampus, the expression of ARHGAP12 was still detectable but remarkably decreased compared to E18 hippocampus (Figure 1C). These results show that ARHGAP12 is expressed in a distinct spatiotemporal pattern within the hippocampus.

The subcellular distribution of Rho GEFs and GAPs is instructive for their function (Govek et al., 2011). We therefore assessed the subcellular distribution of ARHGAP12 in hippocampal CA1 pyramidal neurons. To this end, we tagged ARHGAP12 at its N terminus with GFP and introduced GFP-*Arhgap12*, together with a red fluorescent protein (dsRed) as a cellular marker, into CA1 cells in 12 days in vitro (DIV) organotypic hippocampal slices by biolistic transfection. The partition of ARHGAP12 between spines and dendrites was calculated from the ratio of the GFP and dsRed signal in the spine head versus the adjacent dendritic shaft (Nadif Kasri et al., 2009). We found a strong enrichment of ARHGAP12 in the spines compared to the dendrites (Figure 1D). Consistently, we observed overlapping localization of endogenous ARHGAP12 with postsynaptic density-95 (PSD95) in the stratum radiatum of the hippocampal CA1 region (Figure 1E). Finally, we showed that ectopically expressed GFP-ARHGAP12 colocalized with PSD95 and was found juxtaposed to the presynaptic marker Synapsin-1 in hippocampal primary neurons (Figure S1). Together, these data reveal that ARHGAP12 is located postsynaptically in excitatory synapses of hippocampal CA1 pyramidal neurons.

Negative Regulation of Spine Morphology by ARHGAP12

Given the presence of ARHGAP12 in spines, and the importance of Rho GTPases in controlling actin cytoskeleton remodeling, we first examined the role of ARHGAP12 in regulating dendritic spine morphology in CA1 pyramidal neurons. We biolistically introduced a GFP-expressing construct, as a cellular marker, with or without a second construct containing *Arhgap12* into CA1 neurons in organotypic hippocampal slices. Immunostaining experiments revealed that neurons transfected with GFP alone showed ARHGAP12 levels similar to those of adjacent non-transfected neurons, whereas neurons expressing *Arhgap12* exhibited a 10-fold increase in ARHGAP12 levels (Figure S2B). Compared to neurons expressing GFP alone, *Arhgap12*-overexpressing CA1 pyramidal neurons displayed a significant decrease in both spine density and volume (spine density—GFP control: 5.02 ± 0.22 spines/10 μm, *Arhgap12*: 1.87 ± 0.44 spines/10 μm; spine volume—GFP control: 270.56 ± 49.22 a.u., *Arhgap12*: 153.03 ± 52.68 a.u.; Figures 2A–2C). In addition, we found that elevated ARHGAP12 levels significantly increased the percentage of immature spines in CA1 neurons (GFP control: 6.03% ± 1.05%; *Arhgap12*: 15.90% ± 3.45%; Figure 2D). These observations are consistent with experiments in which reduced Rac1 activity has been coupled to reduced spine density and size (Haditsch et al., 2009).

We next examined the function of endogenous ARHGAP12 by probing the effects of reduced ARHGAP12 expression on dendritic spines. Constructs were generated to co-express GFP and short hairpin RNAs (shRNAs) targeting either the 3′ UTR (*Arhgap12* sh#1) or the translated region (*Arhgap12* sh#2) of rat *Arhgap12* mRNA. *Arhgap12* shRNAs significantly reduced endogenous ARHGAP12 protein levels in hippocampal primary neurons (Figure S2A), as well as in organotypic hippocampal slices (Figure S2B). We found that neither shRNA (*Arhgap12* sh#1 and #2) affected spine density (GFP control: 5.02 ± 0.22 spines/10 μm; *Arhgap12* sh#1: 5.06 ± 0.62 spines/10 μm; *Arhgap12* sh#2: 5.02 ± 1.41 spines/10 μm), but both significantly

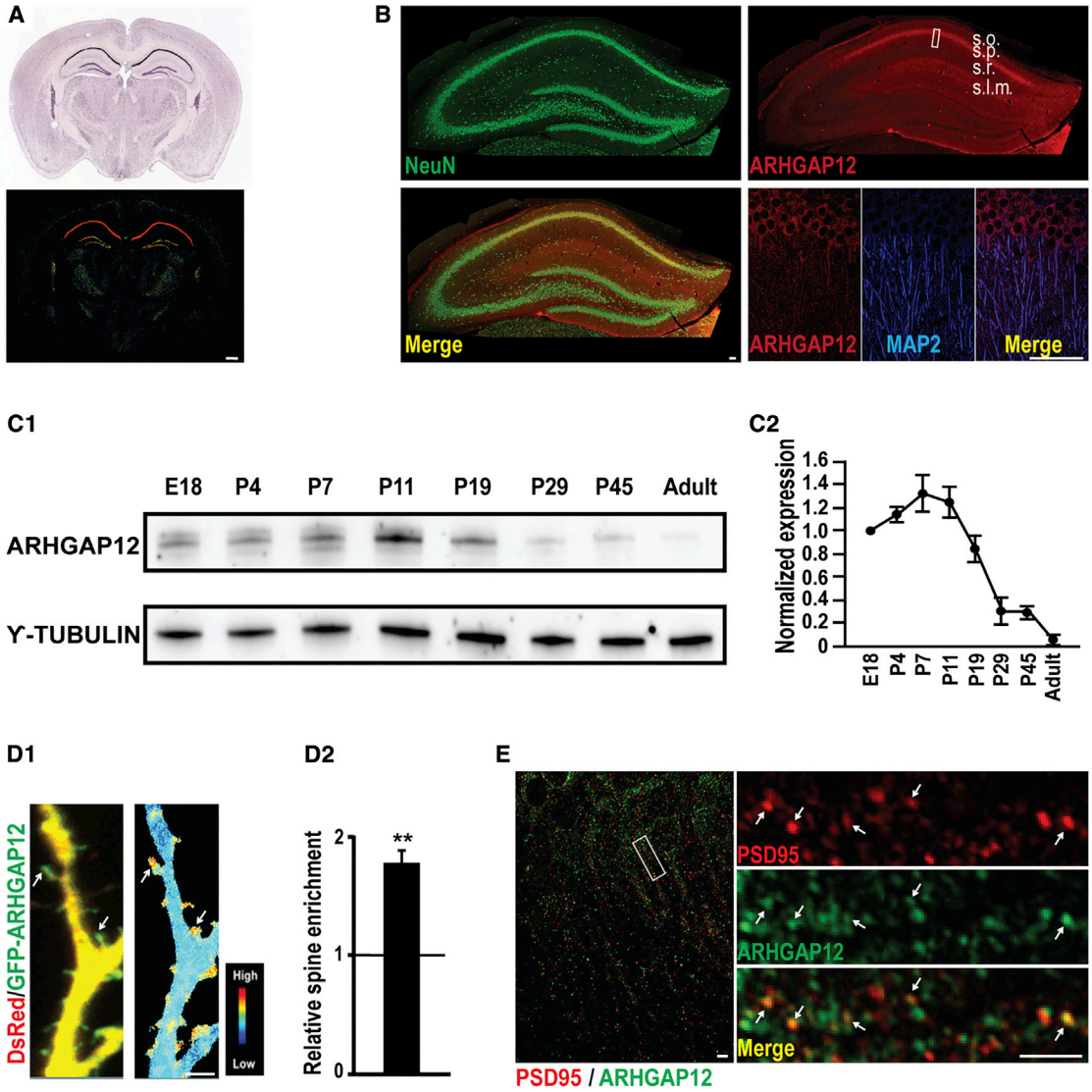

Figure 1. Expression and Distribution of ARHGAP12 in the Hippocampus

(A) In situ hybridization of *Arhgap12* from the Allen Brain Atlas database. Scale bars, 50 μm.

(B) Hippocampi sections from a P20 rat double-immunolabeled with an anti-ARHGAP12 antibody (red) and an anti-NeuN antibody (green). Scale bars, 50 μm.

(C_1) Rat hippocampi collected at indicated ages and probed with anti-ARHGAP12 antibody. Expression of γ-tubulin was used as a loading control; equal amounts of protein (50 μg) were loaded.

(C_2) Quantification of ARHGAP12 proteins levels at indicated postnatal ages. ARHGAP12 expression was normalized to γ-tubulin in the same sample. Data are shown as mean ± SEM; n = 3.

(D_1) Left: representative images of a dendritic branch of a hippocampal CA1 pyramidal neuron co-transfected with GFP-*Arhgap12* (green) and dsRed (red). Right: ratio image of the representative cell. Blue depicts low ARHGAP12 enrichment, and red depicts high density. Scale bar, 5 μm.

(D_2) Quantification of GFP-ARHGAP12 enrichment in spines. Data are shown as mean ± SEM; n = 8; $^{**}p < 0.01$, t test.

(E) Left: hippocampi sections from a P20 rat double-immunolabeled with an anti-ARHGAP12 antibody (green) and an anti-PSD95 antibody (red). Right: higher magnification images of the area indicated in the white box on the left panel. White arrows indicate sites of co-localization of ARHGAP12 and PSD95. Scale bars, 10 μm.

See also Figure S1.

increased spine volume (GFP control: 270.56 ± 49.22 a.u.; *Arhgap12* sh#1: 443.69 ± 52.30 a.u.; *Arhgap12* sh#2: 416.79 ± 116.03 a.u.; Figures 2B and 2C). The percentage of immature spines also significantly decreased in neurons expressing *Arhgap12* shRNAs (GFP control: 6.03% ± 1.05%; *Arhgap12* sh#1: 1.33% ± 1.34%; *Arhgap12* sh#2: 1.68% ± 1.42%; Figure 2D). We were able to rescue these phenotypes by co-expressing *Arhgap12* sh#1 with an *Arhgap12*-expressing vector that lacked the 3′ UTR and was therefore resistant to *Arhgap12* sh#1-mediated knockdown. This confirmed that the knockdown

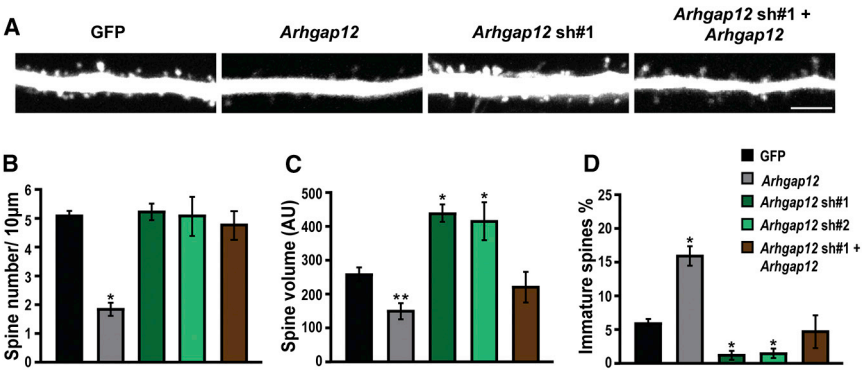

Figure 2. ARHGAP12 Negatively Regulates Spine Morphology

(A) Representative images of secondary apical dendrites from CA1 neurons transfected with indicated constructs. Scale bars, 10 μm.

(B–D) Quantification of spine density (B), spine volume (C), and percentage of immature spines (D) for indicated experimental conditions. Data are shown as mean ± SEM; GFP: n = 15, *Arhgap12*: n = 9, *Arhgap12* sh#1: n = 8, *Arhgap12* sh#2: n = 7, *Arhgap12* sh#1 + *Arhgap12*: n = 9; data from three to four independent experiments. A minimum of 500 spines were analyzed per condition; *p < 0.05, **p < 0.01, one-way ANOVA.

See also Figures S2 and S3.

effects were mediated specifically by loss of ARHGAP12 (spine density—GFP control: 5.02 ± 0.22 spines/10 μm, *Arhgap12* sh#1 + *Arhgap12*: 4.77 ± 1.02 spines/10 μm; spine volume—GFP control: 270.56 ± 49.22 a.u., *Arhgap12* sh#1 + *Arhgap12*: 226.51 ± 103.55 a.u.; Figures 2B–2D). Immunostaining experiments on biolistically transfected organotypic hippocampal slices confirmed that the levels of ARHGAP12 were restored to normal levels (Figure S2B).

Next, we examined whether the regulation of ARHGAP12 on spine morphology was dependent on activity. To this end, we treated organotypic slices with a high concentration of $MgCl_2$ or the N-methyl-D-aspartate receptor (NMDAR) antagonist 2-amino-5-phosphonovaleric acid (APV, 100 μM) on the same day of biolistic transfection. Both manipulations, however, did not prevent the enlargement of spine volume induced by *Arhgap12* downregulation (Figure S3A), indicating that knocking down *Arhgap12* is sufficient to increase spine size. Because the expression of ARHGAP12 declines during normal development, we wondered whether blocking NMDAR activity would affect this process. We found that the gradual decrease of ARHGAP12 levels did not occur in the presence of APV (Figure S3C), suggesting that the developmental elimination of ARHGAP12 is dependent on NMDAR activity.

Together, our results support a model in which NMDAR activity during development drives the repression of ARHGAP12, resulting in the enlargement of spines.

Selective Modulation of Synaptic AMPAR-Mediated Transmission by ARHGAP12

Because of the importance of dendritic spine structure for synaptic function and the effects of ARHGAP12 on spine morphology, we next assessed the role of ARHGAP12 in modulating excitatory synaptic function. We first examined the effects of ARHGAP12 overexpression on synaptic transmission. Simultaneous whole-cell recordings of evoked excitatory postsynaptic currents (EPSCs) were recorded at 7 DIV from CA1 pyramidal neurons expressing GFP-*Arhgap12* and from adjacent non-transfected neurons. Overexpression of *Arhgap12* significantly depressed AMPAR- and NMDAR-mediated synaptic transmission (AMPAR-EPSC—uninfected: 197.61 ± 21.15 pA, infected: 45.33 ± 4.67 pA; NMDAR-EPSC—uninfected: 193.71 ± 19.13 pA, infected: 157.84 ± 18.71 pA; Figures 3A and 3D), suggesting that ectopically expressed *Arhgap12* is sufficient to depress AMPAR- and NMDAR-mediated transmission. Overexpression of GFP alone did not alter AMPAR- or NMDAR-mediated synaptic transmission (Figure S4A). These observations complement our finding that ectopic expression of *Arhgap12* significantly reduced the number of mature spines and therefore could explain the changes in NMDAR-EPSCs, in addition to the changes in AMPAR-EPSCs.

Next, we examined the effects of ARHGAP12 downregulation in regulating synaptic transmission. We found that downregulation of ARHGAP12 levels resulted in potentiation of AMPAR-mediated transmission but not NMDAR-mediated transmission (*Arhgap12* sh#1—AMPAR-EPSC uninfected: 40.03 ± 8.98 pA, AMPAR-EPSC infected: 60.57 ± 7.85 pA, NMDAR-EPSC uninfected: 67.28 ± 7.40 pA, NMDAR-EPSC infected: 72.82 ± 9.94 pA; *Arhgap12* sh#2—AMPAR-EPSC uninfected: 51.32 ± 8.03 pA, AMPAR-EPSC infected: 70.91 ± 5.43 pA, NMDAR-EPSC uninfected: 62.13 ± 8.85 pA, NMDAR-EPSC infected: 67.88 ± 10.62 pA; Figures 3B–3D), indicating that downregulation of ARHGAP12 is sufficient to enhance AMPAR-mediated transmission. These results are consistent with our observation that reducing endogenous ARHGAP12 results in larger dendritic spines without affecting the spine density. Thus, bidirectional manipulation of ARHGAP12 levels is associated with opposing effects toward AMPAR-mediated synaptic transmission.

To test whether the effect of ARHGAP12 on AMPARs is restricted to synaptic AMPARs, we recorded extrasynaptic responses evoked by bath application of AMPA (1 μM), which initiated inward currents in all neurons (Arendt et al., 2010). No differences in AMPA-induced inward currents were observed between control uninfected neurons and *Arhgap12* sh#1 infected neurons (Figure 3E), indicating that the modulation of glutamatergic receptors by ARHGAP12 is specific for synaptic AMPARs. Because altered AMPAR-mediated EPSC may also result from an altered proportion of GluA2-lacking AMPARs, whose currents show unique inward rectification, we further measured the rectification index of AMPAR-EPSCs by measuring AMPAR-mediated EPSCs at −60 and at +40 mV holding potential, in the presence of intracellular spermine (Bowie and Mayer, 1995). However, we did not observe a significant difference between uninfected neurons and *Arhgap12* sh#1 infected neurons (Figure 3F), indicating that

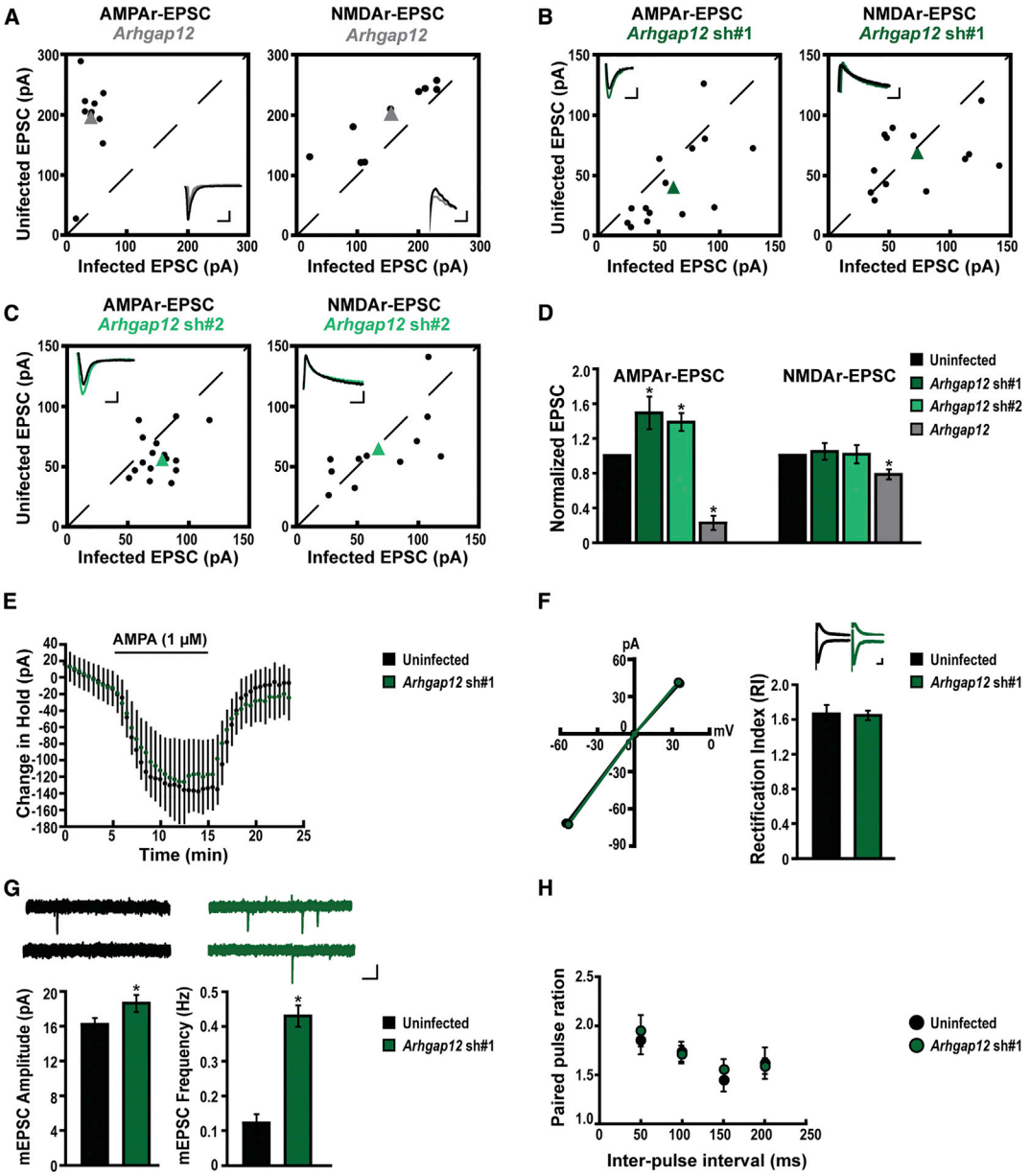

Figure 3. Postsynaptic ARHGAP12 Modulates AMPAR-Mediated Transmission

(A–C) Amplitudes of AMPAR-EPSCs (left panels) and NMDAR-EPSCs (right panels) of uninfected neurons are plotted against simultaneously recorded neighboring neurons expressing *Arhgap12* (A), *Arhgap12* sh#1 (B), and *Arhgap12* sh#2 (C). Recordings were performed at 7 DIV. Black symbols represent single pairs of recordings; green or gray symbols show mean values. Inserts in each panel show sample average traces: black traces, uninfected neurons; gray traces, *Arhgap12*-overexpressed neurons; green traces, *Arhgap12* shRNAs expressing neurons. Scale bars, 10 ms and 25 pA.

(D) Summary of effects of *Arhgap12* overexpression or knockdown. Data are shown as mean ± SEM; n = 9–15 from three independent experiments; *p < 0.05, paired t test.

(E) Time course of whole-cell currents recorded from CA1 pyramidal neurons infected with *Arhgap12* sh#1 or control uninfected neurons during the application of 1 μM AMPA. Uninfected: n = 9, *Arhgap12* sh#1: n = 8; data from two independent experiments.

(F) Synaptic responses were recorded at −60 and +40 mV from CA1 pyramidal neurons infected with *Arhgap12* sh#1 or uninfected neurons in the presence of intracellular spermine. The rectification index was calculated by dividing the amplitude at −60 mV by the amplitude at +40 mV. n = 8 for both conditions from two independent experiments.

(G) Representative traces and quantifications of excitatory miniature events recorded from uninfected neurons and neurons expressing *Arhgap12* sh#1 at 7 DIV. Scale bars, 1 s and 25 pA. Data are shown as mean ± SEM; n = 13–15 from three independent experiments; *p < 0.05, t test.

(H) Paired-pulse facilitation ($EPSC_2/EPSC_1$) recorded from uninfected and *Arhgap12* sh#1-expressing neurons at indicated inter-stimulus intervals. Data are shown as mean ± SEM; n = 7 for both groups from three independent experiments.

See also Figure S4.

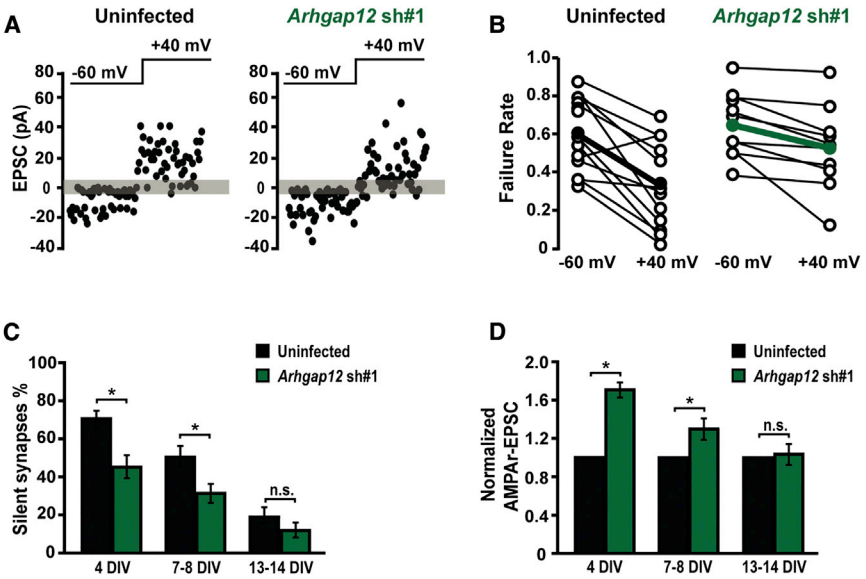

Figure 4. *Arhgap12* Knockdown Promotes Hippocampal Synaptic Development by Accelerating Silent Synapse Unsilencing

(A) Minimal stimulation assay. Representative plot of individual responses at −60 and +40 mV with minimal stimulations in indicated conditions.

(B) Failures of responses using minimal stimulation at −60 and +40 mV from uninfected neurons and *Arhgap12* sh#1 infected neurons.

(C) Percentage of silent synapses at different developmental stages of uninfected neurons and *Arhgap12* sh#1 infected neurons. Data are shown as mean ± SEM; n = 11–14 from three independent experiments; *p < 0.05, paired t test.

(D) Evoked AMPAR-mediated transmission recorded from CA1 pyramidal neurons infected with *Arhgap12* sh#1 and uninfected neurons at different developmental stages. Data are shown as mean ± SEM; n = 11–15 for both groups at all time points, from three to four independent experiments; *p < 0.05, paired t test.

See also Figure S5.

enhanced AMPAR-EPSCs were not a result of changes in AMPAR subunit composition.

The changes in AMPAR-mediated transmission could result from a change of synaptic AMPARs at individual synapses, a change in the number of functional synapses, or both. To determine the precise mechanism, we measured the effect of ARHGAP12 on the amplitudes and frequencies of miniature excitatory postsynaptic currents (mEPSCs). *Arhgap12* sh#1 largely increased both frequency and amplitude of mEPSCs in CA1 pyramidal neurons (Figure 3G). The change in amplitude supports our previous findings showing that ARHGAP12 affects synaptic AMPAR function. A change in frequency usually reflects a change in the number of active synapses or in the presynaptic release probability. We further examined presynaptic release by measuring the paired-pulse ratio. We did not observe significant differences between uninfected and *Arhgap12* sh#1-expressing neurons (Figure 3H), indicating that no retrograde signaling was involved to alter presynaptic release probability and the changes in frequency reflect a change in the amount of active synapses.

Finally, we evaluated the impact of ARHGAP12 on inhibitory (GABAergic) synaptic function in CA1 pyramidal neurons. Evoked inhibitory postsynaptic currents (IPSCs) were measured on neurons expressing *Arhgap12* sh#1 and adjacent control uninfected neurons on hippocampal slices at 7 DIV. We found that *Arhgap12* knockdown did not affect evoked IPSCs (Figure S4B).

Together, our findings indicate that ARHGAP12 is critical for modulating excitatory, but not inhibitory, synaptic transmission at the postsynaptic terminal in a cell-autonomous way.

Arhgap12 Knockdown Promotes Hippocampal Synaptic Development by Accelerating Silent Synapse Unsilencing

Next, we sought to further delineate the mechanism by which ARHGAP12 restricts synaptic function. We reasoned that a plausible mechanism could involve the regulation of silent synapse activation. Silent synapses refer to those synapses with NMDARs but no functional AMPARs (Hanse et al., 2013), and they can convert to active synapses by AMPAR insertion (also termed unsilencing) during development and/or in response to neuronal activity (Isaac et al., 1995; Kerchner and Nicoll, 2008). In the hippocampus, the proportion of these silent synapses rapidly decreases during the first 2 weeks of postnatal development (Kerchner and Nicoll, 2008). To detect silent synapses, we performed whole-cell patch-clamp recordings on CA1 pyramidal neurons using minimum stimulation. In control uninfected 4 DIV CA1 neurons, the failure rate was much larger at −60 mV than at +40 mV (Figures 4A and 4B), indicating that a substantial fraction of the synapses is still silent at this stage of development (Figure 4C). As expected, the proportion of silent synapses gradually decreased during development, with almost all synapses unsilenced at 14 DIV (Figure 4C). When the same experiments were performed on *Arhgap12* sh#1-expressing hippocampal CA1 neurons, we found that the proportion of silent synapses was significantly decreased at the earlier developmental time points (4 and 7–8 DIV) but was comparable to control at 13–14 DIV (Figure 4C), suggesting that *Arhgap12* downregulation promotes synaptic maturation by accelerating synapse unsilencing.

Robust synaptogenesis occurs during the first 2 weeks of postnatal development, and a major mechanism underlying these critical events is synapse unsilencing. Because the developmental gradient of ARHGAP12 expression is inversely correlated to the trend of synaptic maturation in hippocampus, we speculated that ARHGAP12 might act as an endogenous "brake" during development. Namely, decreasing levels of ARHGAP12 would release repression and accelerate synaptogenesis and functional synapse maturation. If this is the case, the potentiation of CA3-CA1 synapses would be stronger when *Arhgap12* is downregulated in the early developmental stages compared to that at the later stages. Conversely, keeping ARHGAP12 expression at a high level throughout development would severely limit excitatory

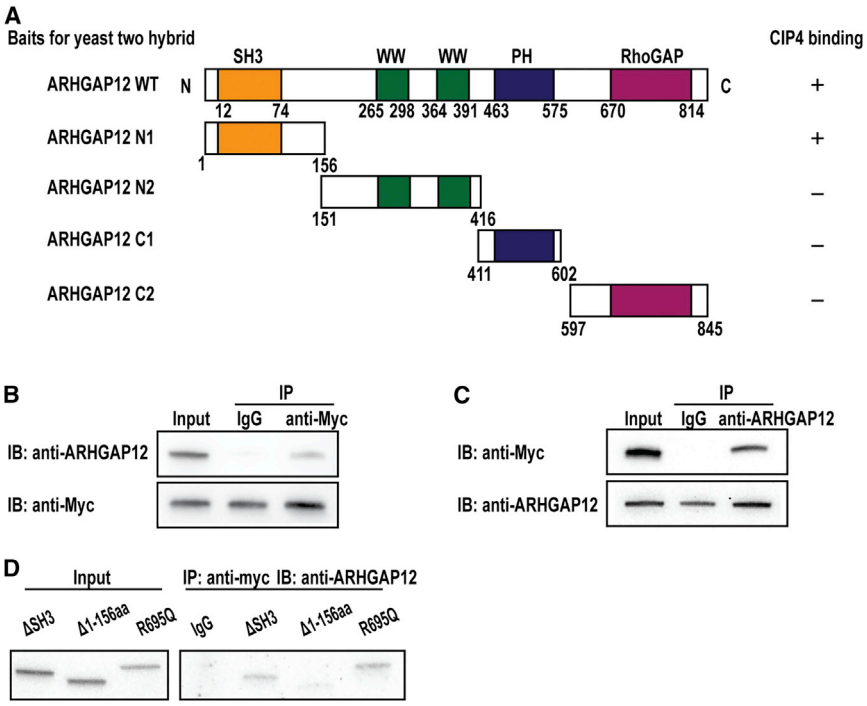

Figure 5. Interaction of ARHGAP12 with CIP4

(A) Domain structure of ARHGAP12 and fragments used as bait in yeast two-hybrid screening. Presence or absence of positive colonies using distinct bait was indicated with + or −, respectively.

(B and C) CoIP of ARHGAP12 and CIP4 in vitro. Protein extract from HEK293T cells co-transfected with GFP-*Arhgap12* and myc-*Cip4* constructs for 24 hr was incubated with mouse immunoglobulin G or with an anti-Myc antibody (B) or an anti-ARHGAP12 antibody (C). The immunoprecipitates were analyzed by immunoblotting using indicated antibodies. n = 6.

(D) CoIP of ARHGAP12 mutants and CIP4 in vitro. Extract from HEK293T cells co-transfected with myc-*Cip4* and indicated mutants of *Arhgap12* for 24 hr was incubated with an anti-CIP4 antibody. Immune complexes were immunoblotted with an anti-ARHGAP12 antibody. n = 3.

synapse development. We first tested this hypothesis by knocking down *Arhgap12* in organotypic hippocampal slices, and we compared evoked AMPAR-EPSC on a CA1 pyramidal neuron expressing *Arhgap12* sh#1 and an adjacent uninfected neuron at different stages of the development (4, 7–8, and 13–14 DIV). Whole-cell patch-clamp recordings revealed that neurons expressing *Arhgap12* sh#1 displayed the most profound potentiation of AMPAR-EPSC at 4 DIV and this effect gradually decreased when recording at later stages, with no changes observed at 13–14 DIV (Figure 4D). Conversely, when keeping elevated levels of ARHGAP12 throughout the development of hippocampal neurons, we observed significantly decreased AMPAR-mediated synaptic transmission, measured as a reduction in amplitude and frequency of mEPSCs (Figures S5A and S5B). The decreased AMPAR-mediated transmission was accompanied by a reduction in PSD95 density, further suggesting that ARHGAP12 can prevent excitatory synapse formation (Figure S5C).

Together, our results indicate that endogenous ARHGAP12 dampens synaptic development by limiting the unsilencing of silent synapses and suggest that endogenous ARHGAP12 acts as a synaptic brake during hippocampal development.

Identification of CIP4 as an ARHGAP12 Interactor

Next, to gain insights into the mechanisms by which ARHGAP12 modulates synapses, we sought to identify direct interactors of ARHGAP12 by performing a GAL4-based interaction trap screen in yeast (yeast two-hybrid system).

ARHGAP12 contains several protein motifs: a Src homology-3 (SH3) domain at its N terminus, two WW domains, and a Pleckstrin-homology (PH) domain, followed by a GAP domain shown to negatively regulate Rac1 GTPase (Gentile et al., 2008). Full-length human ARHGAP12 and fragments containing different conserved domains were used as bait in the yeast two-hybrid screening (Figure 5A). Four independent cDNAs matched the sequence of Cdc42-interacting protein 4 (CIP4, also named thyroid hormone receptor 10 variant; Figure S7A), which harbors a highly conserved F-BAR (Fes-CIP4 homology-Bin/Amphyphysin/Rvsp) domain at the N terminus and has recently been implicated in neurite outgrowth (Saengsawang et al., 2012), clathrin-mediated endocytosis, endosomal trafficking (Itoh and De Camilli, 2006; Shimada et al., 2007; Tsujita et al., 2006), and synaptic growth at the neuromuscular junction (NMJ) in *Drosophila* (Nahm et al., 2010). We subsequently performed co-immunoprecipitation (coIP) experiments to validate the interaction between ARHGAP12 and CIP4. Because none of the antibodies for CIP4 that we have tested to date were suitable for western blot analysis and IP in vivo (data not shown; Saengsawang et al., 2012), we co-expressed GFP-*Arhgap12* wild-type (WT) and Myc-*Cip4* in HEK293T cells and carried out reciprocal coIP experiments using an anti-Myc and an anti-ARHGAP12 antibody. ARHGAP12 specifically co-immunoprecipitated with CIP4, and vice versa (Figures 5B and 5C).

Next, we set out to identify the CIP4 binding region in ARHGAP12. Given that the positive clones from the yeast two-hybrid screening encompassed the first 156 amino acids (aa) of ARHGAP12 (Figure 5A), we reasoned that ARHGAP12 is likely to bind to CIP4 via its N-terminal domain. To test this hypothesis, we generated an ARHGAP12 deletion mutant lacking aa 1–156 (Δ1–156aa) and repeated the coIP experiment. We found that the Δ1–156aa mutant failed to bind CIP4. Because the first 156 aa of ARHGAP12 include an SH3 domain and this domain is known to be critical for protein-protein interactions, we reasoned that ARHGAP12 is likely to bind CIP4 via its SH3 domain. A deletion of the SH3 domain (ΔSH3) of ARHGAP12 was generated and tested for its ability to interact

with full-length CIP4 in HEK293T cells using coIP. Surprisingly, the ΔSH3 mutant of ARHGAP12 was still able to bind CIP4, indicating that the SH3 domain of ARHGAP12 is not required for interacting with CIP4. Likewise, a point mutation leading to an inactivation of the GAP function of ARHGAP12 (R695Q; Figure S6A; Nadif Kasri et al., 2009) did not affect the ARHGAP12-CIP4 interaction in vitro. Overall, these data indicate that ARHGAP12 can interact with CIP4 via its N-terminal domain (aa 1–156).

Functional Dissection of ARHGAP12 Controlling Synaptic Structure and Strength

Previously, ARHGAP12 has been shown to contain a GAP domain that negatively regulates the activity of Rac1 GTPase in non-neuronal cells (Gentile et al., 2008). We confirmed that this is also the case in hippocampal neurons by performing Rac1 activity assay (Figure S6A).

Because ARHGAP12 also interacts with CIP4 via its N-terminal domain, which has been shown to play a role in clathrin-mediated endocytosis (Itoh and De Camilli, 2006; Shimada et al., 2007; Tsujita et al., 2006), we wondered whether these two distinct domains play separate roles affecting synaptic structure and function, respectively. As a first step toward addressing this question, we compared the effects of regulating dendritic spine morphology between ARHGAP12 WT and two mutants, *Arhgap12*_R596Q and *Arhgap12*_Δ1–156aa. Spine structure analysis revealed that expression of the *Arhgap12*_R596Q mutant in CA1 pyramidal neurons failed to mimic the phenotype observed by expressing *Arhgap12* WT, namely, decreased spine density and volume compared to GFP control (spine density—GFP control: 4.62 ± 0.51 spines/10 μm, *Arhgap12* WT: 2.21 ± 0.82 spines/10 μm, *Arhgap12*_R596Q: 4.17 ± 0.36 spines/10 μm; spine volume—GFP control: 273.72 ± 57.27 a.u., *Arhgap12* WT: 150.11 ± 52.73 a.u., *Arhgap12*_R596Q: 307.61 ± 35.2 a.u.; Figures 6A and 6B). Conversely, *Arhgap12*_Δ1–156aa-expressing CA1 neurons displayed spine morphology similar to *Arhgap12* WT-expressing neurons (spine density—GFP control: 4.62 ± 0.51 spines/10 μm, *Arhgap12* WT: 2.21 ± 0.82 spines/10 μm, *Arhgap12*_ Δ1–156aa: 2.41 ± 0.78 spines/10 μm; spine volume—GFP control: 273.72 ± 57.27 a.u., *Arhgap12* WT: 150.11 ± 52.73 a.u., *Arhgap12*_Δ1–156aa: 175.45 ± 53.01 a.u.; Figures 6A and 6B). These data indicate that the GAP activity of ARHGAP12, but not its interaction with CIP4, is required to regulate dendritic spine morphology. To corroborate our data showing ARHGAP12 affects dendritic spine structure by acting on the Rac1 signaling pathway, we examined whether inhibiting Rac1 signaling could rescue the increased spine volume resulting from *Arhgap12* knockdown by using the competitive inhibitor of Rac1 activation NSC23766 (Gao et al., 2004). We found that NSC23766 (0.1 mM) treatment of *Arhgap12* shRNA transfected hippocampal slices largely rescued the spine volume defects in *Arhgap12* knockdown neurons. The mean spine volume did not significantly increase compared to control GFP-expressed neurons (spine density—GFP control: 4.62 ± 0.51 spines/10 μm, *Arhgap12* sh#1: 5.06 ± 0.62 spines/10 μm, *Arhgap12* sh#1 + Rac1 inhibitor: 4.34 ± 0.75 spines/10 μm; spine volume—GFP control: 273.72 ± 57.27 a.u., *Arhgap12* sh#1: 443.69 ± 52.30 a.u., *Arhgap12* sh#1 + Rac1 inhibitor: 251.54 ± 73.82 a.u.; Figures 6A and 6B). Moreover, we found that, as expected, treating neurons with NSC23766 resulted in decreased spine density and volume, and this treatment on *Arhgap12*-overexpressed neurons did not cause additional effects on spine morphology (Figures S6B and S6C). Overall, these findings imply that the GAP activity of ARHGAP12, but not ARHGAP12-CIP4 interaction, is responsible for controlling dendritic spine morphology in CA1 pyramidal neurons via the Rac1 GTPase signaling pathway.

Given that CIP4 is involved in clathrin-dependent endocytosis, a mechanism that mediates internalization of most plasma membrane proteins, including AMPARs (Man et al., 2000), we speculated that the inhibitory effect of ARHGAP12 on AMPAR function could be due to involvement of the ARHGAP12-CIP4 complex in AMPAR endocytosis process. To directly evaluate the AMPAR endocytotic process, live-cell antibody feeding experiments were performed in 14 DIV primary hippocampal neurons transfected with GFP, *Arhgap12* sh#1, *Arhgap12* WT, *Arhgap12*_R695Q, or *Arhgap12*_Δ1–156aa. We observed impaired GluA1 endocytosis in neurons expressing *Arhgap12* sh#1. Both *Arhgap12* WT and *Arhgap12*_R695Q significantly enhanced endocytosis of GluA1 compared to the GFP control condition, whereas the *Arhgap12*_Δ1–156aa mutant did not alter GluA1 endocytosis (Figure 6C). Functionally, overexpression of *Arhgap12* WT decreased both mEPSC amplitude and frequency. *Arhgap12*_R695Q overexpression led to reduced mEPSC amplitude without affecting frequency, whereas *Arhgap12*_Δ1–156aa resulted in unaltered amplitude but reduced frequency (Figures 6D and 6E).

Furthermore, based on the minimal interacting sequence (414–428 aa) in CIP4 that we obtained from our yeast two-hybrid screening (Figure S7A), we designed a small interfering peptide ($Pep^{A12\text{-}CIP4}$) to disrupt the ARHGAP12-CIP4 complex. A corresponding scrambled peptide was used as a control (Pep^{ctrl}). The peptides were conjugated to the cell-membrane transduction domain of the HIV-1 TAT protein, which allowed the peptide to cross the membrane of neurons. In HEK293T cells, we found that $Pep^{A12\text{-}CIP4}$ disrupted the ARHGAP12-CIP4 interaction, whereas Pep^{ctrl} did not (Figure 7A). In addition, we observed no effect of both Pep^{ctrl} and $Pep^{A12\text{-}CIP4}$ on surface NMDAR expression and Cdc42-CIP4 interaction (Figures S7B and S7C). Next, we examined whether disrupting the ARHGAP12-CIP4 interaction influences GluA1 endocytosis. Live-cell antibody feeding experiments were performed in 14 DIV primary hippocampal neurons treated with Pep^{ctrl} or $Pep^{A12\text{-}CIP4}$ for 24 hr. Our results showed that $Pep^{A12\text{-}CIP4}$ significantly impaired AMPAR GluA1 subunit endocytosis compared to Pep^{ctrl}-treated neurons (Figure 7B). Electrophysiologically, CA1 pyramidal neurons treated with $Pep^{A12\text{-}CIP4}$ exhibited significantly increased amplitude compared to Pep^{ctrl}-treated neurons (Figure 7C). This indicated that disrupting the interaction of ARHGAP12-CIP4 was sufficient to increase the amount of AMPARs accumulating at synapses, mimicking the effect of ARHGAP12 knockdown on AMPAR-mediated transmission. Finally, to further exclude the possibility that the ARHGAP12-CIP4 interaction can regulate spine morphology, we imaged dendritic spine morphology of neurons treated with Pep^{ctrl} or $Pep^{A12\text{-}CIP4}$. No significant differences between the two conditions were

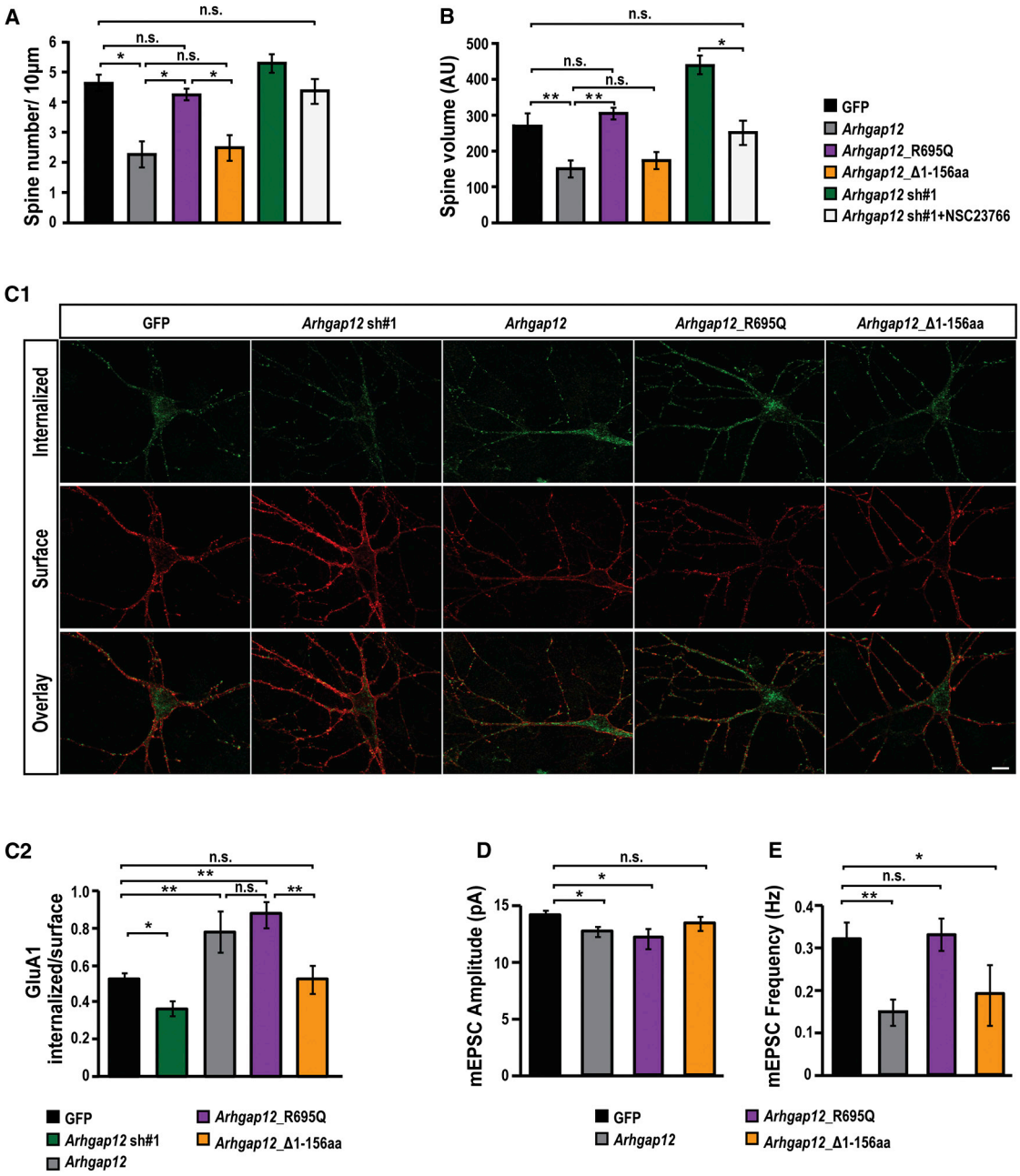

Figure 6. ARHGAP12 Regulates Synaptic Structure and Function via Distinct Domains

(A and B) Morphological analysis of dendritic spine density (A) and volume (B) of CA1 pyramidal neurons in indicated conditions. Data are shown as mean ± SEM; GFP: n = 15, *Arhgap12*: n = 9, *Arhgap12*_R695Q: n = 9, *Arhgap12*_Δ1–156aa: n = 8, *Arhgap12* sh#1 + NSC23766: n = 6; data pooled from three to four independent experiments; *p < 0.05, **p < 0.01, one-way ANOVA.

(C) AMPAR endocytosis assay. (C_1) Representative double-labeled images of the internalized (green) and surface (red) AMPAR GluA1 subunit in low-density 14 DIV hippocampal neurons in indicated experimental groups. (C_2) Ratiometric analysis of the intensity of internalized GluA1 to surface GluA1 in indicated conditions. Data are shown as mean ± SEM; control: n = 34, *Arhgap12* sh#1: n = 20, *Arhgap12*: n = 15, *Arhgap12*_R695Q: n = 15, *Arhgap12*_Δ1–156aa: n = 15; data pooled from three independent cultures; *p < 0.05, t test. Scale bars, 10 µm.

(D and E) Excitatory miniature events recorded from neurons biolistically transfected at 12 DIV with indicated constructs. Data are shown as mean ± SEM; GFP: n = 12, *Arhgap12*: n = 16, *Arhgap12*_R695Q: n = 11, *Arhgap12*_Δ1–156aa: n = 11; data pooled from three independent experiments; *p < 0.05, **p < 0.01, one-way ANOVA.

See also Figure S6.

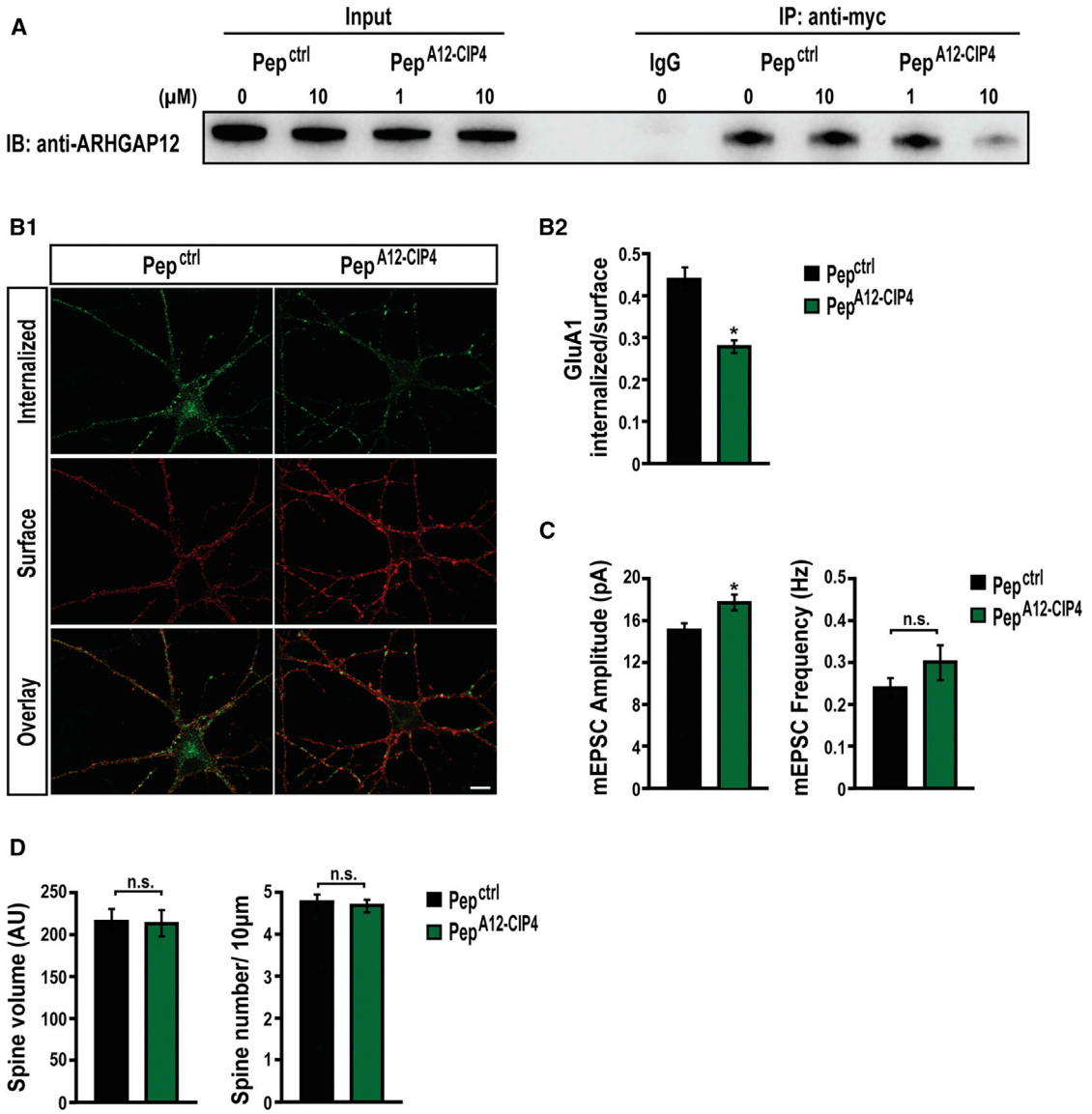

Figure 7. Disrupting ARHGAP12-CIP4 Interaction Impairs AMPAR Endocytosis

(A) HEK293T cells co-transfected with GFP-*Arhgap12* and myc-*Cip4* constructs were incubated with Pep^{ctrl} and $Pep^{ARHGAP12\text{-}CIP4}$ with indicated concentrations for 24 hr. Interaction between ARHGAP12 and CIP4 were examined using immunoblotting with an anti-ARHGAP12 antibody. n = 3.

(B) AMPAR endocytosis assay. (B_1) Representative double-labeled images of the internalized (green) and surface (red) AMPAR GluA1 subunit in low-density 14 DIV hippocampal neurons. (B_2) Ratiometric analysis of the intensity of internalized GluA1 to surface GluA1 in Pep^{ctrl} and $Pep^{ARHGAP12\text{-}CIP4}$ conditions. Data are shown as mean ± SEM; Pep^{ctrl}: n = 18, $Pep^{ARHGAP12\text{-}CIP4}$: n = 19; data pooled from three independent cultures; *$p < 0.05$, t test. Scale bar, 10 μm.

(C) Excitatory miniature events recorded at 14 DIV from organotypic hippocampal slices treated with Pep^{ctrl} or $Pep^{ARHGAP12\text{-}CIP4}$ for 24 hr. Data are shown as mean ± SEM; Pep^{ctrl}: n = 13, $Pep^{ARHGAP12\text{-}CIP4}$: n = 12; data pooled from three independent experiments; *$p < 0.05$, t test.

(D) Morphological analysis of dendritic spine density and volume of CA1 pyramidal neurons treated with 10 μM Pep^{ctrl} or 10 μM $Pep^{ARHGAP12\text{-}CIP4}$ for 24 hr. Data are shown as mean ± SEM; Pep^{ctrl}: n = 7, $Pep^{ARHGAP12\text{-}CIP4}$: n = 7; data from three independent experiments; t test.

See also Figure S7.

observed (Figure 7D). These results suggest that the ARHGAP12-CIP4 interaction is responsible for controlling AMPAR endocytosis but not for regulating spine morphology.

Together, our findings indicate that ARHGAP12 regulates spine morphology via its GAP activity and synaptic strength via its interaction with the F-BAR protein CIP4.

DISCUSSION

The molecular mechanisms that promote excitatory synapse formation and maturation have been extensively studied. However, the molecular events preventing precocious excitatory synapse development so that synapses form at the correct time and

place are less well understood. Here, we identified ARHGAP12, a previously uncharacterized Rac1 GAP in the brain, as a critical coordinator of synaptic structure and function in the developing hippocampus.

ARHGAP12-Rac1 Signaling in Regulating Spine Morphology

In the present study, we focused on hippocampal CA3-CA1 synapses, based on the prominent expression of ARHGAP12 in CA1 during early development. We found that overexpressing WT *Arhgap12* resulted in reduced spine density and volume, and an increased percentage of immature spines in CA1 pyramidal neurons, whereas overexpressing the *Arhgap12* GAP mutant failed to generate a similar phenotype. In addition, we showed that downregulation of *Arhgap12* led to enlarged spine volume and this enlargement was successfully rescued by pharmacologically inhibiting overactive Rac1 signaling. These results strongly suggest that negatively regulating Rac1 signaling via ARHGAP12's GAP activity is essential for maintaining the normal dendritic spine structure at the CA3-CA1 synapse. These data agree with several other reports in which downregulation or overexpression of Rac1 GAPs increased or decreased spine size and density, respectively (Tolias et al., 2011). For instance, overexpression of the Rac1 GAP, alpha 1-chimerin, resulted in a loss of spines by inhibiting the formation of new spines, as well as promoting the pruning of existing spines (Buttery et al., 2006; Van de Ven et al., 2005). More recently, mice lacking the RacGAP Bcr and its relative Abr were shown to exhibit increased spine size and density (Um et al., 2014).

An intriguing aspect of our study is that ARHGAP12 exhibits a unique spatiotemporal profile, with almost exclusive expression in CA1 and DG. Specific spatiotemporal profiles have been observed for numerous GEFs and GAPs and are believed to contribute to the specificity of Rho signaling in the brain (Tolias et al., 2011). Our study thus unveils a vital role of ARHGAP12 in regulating spine structure via Rac1 signaling in CA1 and supports the hypothesis that Rho GEFs and GAPs cooperate in complementary signaling pathways to spatially and temporally regulate Rho GTPase signaling during synapse remodeling (Duman et al., 2015)

ARHGAP12-CIP4 Interaction in Regulating Synaptic Strength

In this study, we found that knocking down *Arhgap12* potentiated hippocampal CA3-CA1 synapses, whereas *Arhgap12* upregulation led to significant synaptic depression. Specifically, *Arhgap12* knockdown increased AMPAR-mediated EPSCs and the frequency and amplitude of mEPSCs, indicating that reducing ARHGAP12 levels promoted synaptic expression of AMPARs. Due to the tight correlation between synaptic strength and spine size, the increase in synaptic strength could occur as a consequence of the changes in spine size (Matsuzaki et al., 2001; Nimchinsky et al., 2002). Alternatively, ARHGAP12 could regulate synapse function independently of spine size. We found that the F-BAR-containing protein CIP4 interacts with ARHGAP12. Similar to ARHGAP12, CIP4 is highly expressed during early cortical development, and CIP4 inhibits neurite formation by promoting lamellipodial protrusions (Saengsawang et al., 2012) and restrains synaptic growth at the NMJ (Nahm et al., 2010). We demonstrated that the interaction between ARHGAP12 and CIP4 involves the N terminus of ARHGAP12 and is independent of its GAP activity. CIP4 is recruited in clathrin-coated pits during clathrin-mediated endocytosis (Shimada et al., 2007), implying a function for CIP4 in this process. We showed that interrupting the ARHGAP12-CIP4 interaction, using a peptide mimicking the ARHGAP12 binding site on CIP4, resulted in elevated AMPAR-mediated transmission. In addition, interfering with the ARHGAP12-CIP4 interaction decreased the endocytosis of GluA1 AMPAR subunits, leading to more synaptic AMPARs. We found that the interaction between ARHGAP12 and CIP4 was not required for regulating spine morphology. This is somewhat different from the function of CIP4 at the NMJ in *Drosophila*, where dCIP4 acts downstream of Cdc42 to activate the postsynaptic Wsp-Arp2/3 pathway and thus restrain synaptic growth (Nahm et al., 2010). Together, these data suggest that by binding to CIP4, ARHGAP12 increases AMPAR endocytosis and thereby reduces synaptic strength. Several studies have shown that events triggering changes spine morphology and insertion or removal of AMPAR subunits are distinct. How these two events are kept in check so that changes in spine morphology correlate with synaptic strength is still unclear. The GluA1 C-tail has been proposed to play a critical role herein by linking both events (Kopec et al., 2006). Our data unveil an interesting model in which ARHGAP12, via its GAP activity, regulates spine structure, while by interacting with CIP4, ARHGAP12 is able to modulate AMPAR-mediated synaptic transmission in the hippocampus. Thus neurons might use an elegant mechanism to keep changes in spine morphology and synaptic strength balanced, where ARHGAP12 signaling controls both actin polymerization and AMPAR trafficking. Exactly how ARHGAP12 and CIP4 cooperate to increase AMPAR endocytosis remains to be elucidated. It is possible that CIP4, similar to FBP17, affects AMPAR endocytosis by recruiting Wiskott-Aldrich syndrome protein and dynamin for vesicle initiation and scission (Shimada et al., 2007).

Synaptic Maturation Is Restricted by ARHGAP12 during Hippocampal Development

A characteristic hallmark of the developing brain is the presence of silent synapses, which contain NMDARs but lack AMPARs. Premature or delayed synapse unsilencing has been implicated in neurodevelopmental disorders, including ASD (Clement et al., 2012, 2013; Sasaki et al., 2010). Because ARHGAP12 is highly expressed during early postnatal stages and is followed by a gradual decline in CA1, which mirrors the trend of robust synaptogenesis, it raises the possibility that the presence of ARHGAP12 might impede synaptic development. Our data showed that the potentiation of synaptic transmission, as a result of *Arhgap12* downregulation, was the strongest at 4 DIV and gradually decreased with age. Conversely, when ARHGAP12 was maintained at a high level, synaptic development was impeded. We thus unveil a potentially interesting positive feedback mechanism between synaptic activity and ARHGAP12 signaling in the sense that synaptic activity is required for ARHGAP12 repression and, in turn, ARHGAP12 downregulation enhances synaptic efficacy. Such a positive feedback

relationship could play a key role during critical periods of synapse development, with too little activity preventing synapse development. Our data thus support the notion that ARHGAP12 is an intrinsic factor in the developmental program of synapses and functions as a synaptic brake during hippocampal development. Releasing the braking effect of ARHGAP12 at an inappropriate time might result in mistimed maturation of glutamatergic synapses and in a disrupted balance between excitation and inhibition in the hippocampus.

In addition, several genes associated with ASD have been identified to function like synaptic brakes to prevent precocious maturation of excitatory synapses. In particular, accelerated maturation of excitatory synapses in an early period of hippocampal development has been observed in a mouse model of human *SYNGAP1* haploinsufficiency, leading to learning deficits (Clement et al., 2012). Similarly, accelerated maturation of glutamatergic synapse has been seen in a knockout mouse model for MET receptor tyrosine kinase. Hepatocyte growth factor (HGF) signaling through MET receptor activation prevents the maturation of silent synapses (Qiu et al., 2014). This is of particular interest because ARHGAP12 was initially characterized as a transcriptional target of HGF in epithelial cells (Gentile et al., 2008). In addition, MET is highly expressed in CA1 pyramidal neurons during late prenatal and early postnatal development (Achim et al., 1997; Judson et al., 2009; Thewke and Seeds, 1999), similar to the expression pattern of ARHGAP12. This raises the intriguing possibility that ARHGAP12 might function downstream of MET signaling in the developing hippocampus. Future experiments will have to determine whether and how ARHGAP12 participates in MET signaling during development.

EXPERIMENTAL PROCEDURES

Virus production, western blot, immunofluorescence, yeast two-hybrid screening, and image analysis are described in the Supplemental Experimental Procedures.

Animals

Wistar rats were housed per two or three animals on a 12 hr light cycle in a temperature-controlled (21 ± 1°C) environment with ad libitum access to food and water. Rats were used at E18 or postnatal day 6 (P6) for primary neuronal cultures or organotypic hippocampal slices, respectively. All experiments involving animals were evaluated and approved by the Committee for Animal Experiments of the Radboud University Nijmegen Medical Centre, Nijmegen, the Netherlands.

Electrophysiology

Whole-cell recordings in cultured slices were obtained with Multiclamp 700B amplifiers (Axon Instruments). To study the effects of ARHGAP12 on synaptic transmission, organotypic hippocampal slices were infected with lentiviruses expressing shRNAs on the same day of plating and recorded at indicated times after infection (4, 7, and 13–14 DIV). To overexpress ARHGAP12, organotypic hippocampal slices were biolistically transfected at 5 DIV (for evoked EPSCs) or 12 DIV (for mEPSCs) using a Helios Gene Gun (Bio-Rad) and analyzed 2 days post-transfection. Whole-cell recordings were obtained simultaneously from an infected and an adjacent uninfected neuron in the CA1 region under visual guidance, using epifluorescence and transmitted light illumination. See the Supplemental Experimental Procedures for details.

Two-Photon Laser Scanning Microscopy

Imaging was essentially performed as described previously (Nadif Kasri et al., 2009).

SUPPLEMENTAL INFORMATION

Supplemental Information includes Supplemental Experimental Procedures and seven figures and can be found with this article online at http://dx.doi.org/10.1016/j.celrep.2016.01.037.

AUTHOR CONTRIBUTIONS

Conceptualization, W.B. and N.N.K.; Methodology, W.B., M.M.S., M.B., and S.J.L.; Investigation, W.B., N.N.K., J.v.d.R., H.v.V., L.-L.L., M.J.C., and R.S.E.L.; Resources, A.R.O., R.R., and R.J.A.v.W.; Writing – Original Draft, W.B. and N.N.K.; Writing – Review and Editing, W.B. and N.N.K.; Supervision, H.v.B. and N.N.K.; Funding Acquisition, N.N.K.

ACKNOWLEDGMENTS

We thank Dr. M. Furuse, Dr. E. Dent, and A. Craig for providing ARHGAP12 and CIP4 plasmids and J.M. Keller for proofreading the manuscript. The research of the authors is supported by grants from the Hypatia fellowship award of the Radboudumc (N.N.K.), the FP7-Marie Curie International Reintegration (277091 to N.N.K.), the Jerome Lejeune Foundation (N.N.K.), the Netherlands Organization for Scientific Research (NWO Vici-865.12.005 to R.R. and open ALW ALW2PJ/13082 to H.v.B. and N.N.K.) and GENCODYS, an EU FP7 large-scale integrating project (241995 to H.v.B.).

Received: July 31, 2015
Revised: November 28, 2015
Accepted: January 9, 2016
Published: February 4, 2016

REFERENCES

Achim, C.L., Katyal, S., Wiley, C.A., Shiratori, M., Wang, G., Oshika, E., Petersen, B.E., Li, J.M., and Michalopoulos, G.K. (1997). Expression of HGF and cMet in the developing and adult brain. Brain Res. Dev. Brain Res. *102*, 299–303.

Allen, K.M., Gleeson, J.G., Bagrodia, S., Partington, M.W., MacMillan, J.C., Cerione, R.A., Mulley, J.C., and Walsh, C.A. (1998). PAK3 mutation in nonsyndromic X-linked mental retardation. Nat. Genet. *20*, 25–30.

Arendt, K.L., Royo, M., Fernández-Monreal, M., Knafo, S., Petrok, C.N., Martens, J.R., and Esteban, J.A. (2010). PIP3 controls synaptic function by maintaining AMPA receptor clustering at the postsynaptic membrane. Nat. Neurosci. *13*, 36–44.

Ba, W., van der Raadt, J., and Nadif Kasri, N. (2013). Rho GTPase signaling at the synapse: implications for intellectual disability. Exp. Cell Res. *319*, 2368–2374.

Bowie, D., and Mayer, M.L. (1995). Inward rectification of both AMPA and kainate subtype glutamate receptors generated by polyamine-mediated ion channel block. Neuron *15*, 453–462.

Buttery, P., Beg, A.A., Chih, B., Broder, A., Mason, C.A., and Scheiffele, P. (2006). The diacylglycerol-binding protein alpha1-chimaerin regulates dendritic morphology. Proc. Natl. Acad. Sci. USA *103*, 1924–1929.

Chater, T.E., and Goda, Y. (2014). The role of AMPA receptors in postsynaptic mechanisms of synaptic plasticity. Front. Cell. Neurosci. *8*, 401.

Cingolani, L.A., and Goda, Y. (2008). Actin in action: the interplay between the actin cytoskeleton and synaptic efficacy. Nat. Rev. Neurosci. *9*, 344–356.

Clement, J.P., Aceti, M., Creson, T.K., Ozkan, E.D., Shi, Y., Reish, N.J., Almonte, A.G., Miller, B.H., Wiltgen, B.J., Miller, C.A., et al. (2012). Pathogenic SYNGAP1 mutations impair cognitive development by disrupting maturation of dendritic spine synapses. Cell *151*, 709–723.

Clement, J.P., Ozkan, E.D., Aceti, M., Miller, C.A., and Rumbaugh, G. (2013). SYNGAP1 links the maturation rate of excitatory synapses to the duration of critical-period synaptic plasticity. J. Neurosci. *33*, 10447–10452.

Duman, J.G., Mulherkar, S., Tu, Y.-K., X Cheng, J., and Tolias, K.F. (2015). Mechanisms for spatiotemporal regulation of Rho-GTPase signaling at synapses. Neurosci. Lett. *601*, 4–10.

Engert, F., and Bonhoeffer, T. (1999). Dendritic spine changes associated with hippocampal long-term synaptic plasticity. Nature *399*, 66–70.

Fukazawa, Y., Saitoh, Y., Ozawa, F., Ohta, Y., Mizuno, K., and Inokuchi, K. (2003). Hippocampal LTP is accompanied by enhanced F-actin content within the dendritic spine that is essential for late LTP maintenance in vivo. Neuron *38*, 447–460.

Gao, Y., Dickerson, J.B., Guo, F., Zheng, J., and Zheng, Y. (2004). Rational design and characterization of a Rac GTPase-specific small molecule inhibitor. Proc. Natl. Acad. Sci. USA *101*, 7618–7623.

Gentile, A., D'Alessandro, L., Lazzari, L., Martinoglio, B., Bertotti, A., Mira, A., Lanzetti, L., Comoglio, P.M., and Medico, E. (2008). Met-driven invasive growth involves transcriptional regulation of Arhgap12. Oncogene *27*, 5590–5598.

Govek, E.-E., Hatten, M.E., and Van Aelst, L. (2011). The role of Rho GTPase proteins in CNS neuronal migration. Dev. Neurobiol. *71*, 528–553.

Guerrier, S., Coutinho-Budd, J., Sassa, T., Gresset, A., Jordan, N.V., Chen, K., Jin, W.L., Frost, A., and Polleux, F. (2009). The F-BAR domain of srGAP2 induces membrane protrusions required for neuronal migration and morphogenesis. Cell *138*, 990–1004.

Haditsch, U., Leone, D.P., Farinelli, M., Chrostek-Grashoff, A., Brakebusch, C., Mansuy, I.M., McConnell, S.K., and Palmer, T.D. (2009). A central role for the small GTPase Rac1 in hippocampal plasticity and spatial learning and memory. Mol. Cell. Neurosci. *41*, 409–419.

Hanse, E., Seth, H., and Riebe, I. (2013). AMPA-silent synapses in brain development and pathology. Nat. Rev. Neurosci. *14*, 839–850.

Hichri, H., Rendu, J., Monnier, N., Coutton, C., Dorseuil, O., Poussou, R.V., Baujat, G., Blanchard, A., Nobili, F., Ranchin, B., et al. (2011). From Lowe syndrome to Dent disease: correlations between mutations of the OCRL1 gene and clinical and biochemical phenotypes. Hum. Mutat. *32*, 379–388.

Hotulainen, P., and Hoogenraad, C.C. (2010). Actin in dendritic spines: connecting dynamics to function. J. Cell Biol. *189*, 619–629.

Ip, J.P., Shi, L., Chen, Y., Itoh, Y., Fu, W.Y., Betz, A., Yung, W.H., Gotoh, Y., Fu, A.K., and Ip, N.Y. (2012). α2-chimaerin controls neuronal migration and functioning of the cerebral cortex through CRMP-2. Nat. Neurosci. *15*, 39–47.

Isaac, J.T.R., Nicoll, R.A., and Malenka, R.C. (1995). Evidence for silent synapses: implications for the expression of LTP. Neuron *15*, 427–434.

Itoh, T., and De Camilli, P. (2006). BAR, F-BAR (EFC) and ENTH/ANTH domains in the regulation of membrane-cytosol interfaces and membrane curvature. Biochim. Biophys. Acta *1761*, 897–912.

Judson, M.C., Bergman, M.Y., Campbell, D.B., Eagleson, K.L., and Levitt, P. (2009). Dynamic gene and protein expression patterns of the autism-associated met receptor tyrosine kinase in the developing mouse forebrain. J. Comp. Neurol. *513*, 511–531.

Kerchner, G.A., and Nicoll, R.A. (2008). Silent synapses and the emergence of a postsynaptic mechanism for LTP. Nat. Rev. Neurosci. *9*, 813–825.

Kopec, C., and Malinow, R. (2006). Neuroscience. Matters of size. Science *314*, 1554–1555.

Kopec, C.D., Li, B., Wei, W., Boehm, J., and Malinow, R. (2006). Glutamate receptor exocytosis and spine enlargement during chemically induced long-term potentiation. J. Neurosci. *26*, 2000–2009.

Kutsche, K., Yntema, H., Brandt, A., Jantke, I., Nothwang, H.G., Orth, U., Boavida, M.G., David, D., Chelly, J., Fryns, J.P., et al. (2000). Mutations in ARHGEF6, encoding a guanine nucleotide exchange factor for Rho GTPases, in patients with X-linked mental retardation. Nat. Genet. *26*, 247–250.

Li, Z., and Sheng, M. (2003). Some assembly required: the development of neuronal synapses. Nat. Rev. Mol. Cell Biol. *4*, 833–841.

Malinow, R., and Malenka, R.C. (2002). AMPA receptor trafficking and synaptic plasticity. Annu. Rev. Neurosci. *25*, 103–126.

Man, H.Y., Lin, J.W., Ju, W.H., Ahmadian, G., Liu, L., Becker, L.E., Sheng, M., and Wang, Y.T. (2000). Regulation of AMPA receptor-mediated synaptic transmission by clathrin-dependent receptor internalization. Neuron *25*, 649–662.

Matsuzaki, M., Ellis-Davies, G.C., Nemoto, T., Miyashita, Y., Iino, M., and Kasai, H. (2001). Dendritic spine geometry is critical for AMPA receptor expression in hippocampal CA1 pyramidal neurons. Nat. Neurosci. *4*, 1086–1092.

Matsuzaki, M., Honkura, N., Ellis-Davies, G.C.R., and Kasai, H. (2004). Structural basis of long-term potentiation in single dendritic spines. Nature *429*, 761–766.

McAllister, A.K. (2007). Dynamic aspects of CNS synapse formation. Annu. Rev. Neurosci. *30*, 425–450.

Nadif Kasri, N., and Van Aelst, L. (2008). Rho-linked genes and neurological disorders. Pflugers Arch. *455*, 787–797.

Nadif Kasri, N., Nakano-Kobayashi, A., Malinow, R., Li, B., and Van Aelst, L. (2009). The Rho-linked mental retardation protein oligophrenin-1 controls synapse maturation and plasticity by stabilizing AMPA receptors. Genes Dev. *23*, 1289–1302.

Nadif Kasri, N., Nakano-Kobayashi, A., and Van Aelst, L. (2011). Rapid synthesis of the X-linked mental retardation protein OPHN1 mediates mGluR-dependent LTD through interaction with the endocytic machinery. Neuron *72*, 300–315.

Nahm, M., Kim, S., Paik, S.K., Lee, M., Lee, S., Lee, Z.H., Kim, J., Lee, D., Bae, Y.C., and Lee, S. (2010). dCIP4 (*Drosophila* Cdc42-interacting protein 4) restrains synaptic growth by inhibiting the secretion of the retrograde Glass bottom boat signal. J. Neurosci. *30*, 8138–8150.

Nimchinsky, E.A., Sabatini, B.L., and Svoboda, K. (2002). Structure and function of dendritic spines. Annu. Rev. Physiol. *64*, 313–353.

Okamoto, K., Nagai, T., Miyawaki, A., and Hayashi, Y. (2004). Rapid and persistent modulation of actin dynamics regulates postsynaptic reorganization underlying bidirectional plasticity. Nat. Neurosci. *7*, 1104–1112.

Penzes, P., Cahill, M.E., Jones, K.A., VanLeeuwen, J.E., and Woolfrey, K.M. (2011). Dendritic spine pathology in neuropsychiatric disorders. Nat. Neurosci. *14*, 285–293.

Phillips, M., and Pozzo-Miller, L. (2015). Dendritic spine dysgenesis in autism related disorders. Neurosci. Lett. *601*, 30–40.

Qiu, S., Lu, Z., and Levitt, P. (2014). MET receptor tyrosine kinase controls dendritic complexity, spine morphogenesis, and glutamatergic synapse maturation in the hippocampus. J. Neurosci. *34*, 16166–16179.

Ramachandran, B., and Frey, J.U. (2009). Interfering with the actin network and its effect on long-term potentiation and synaptic tagging in hippocampal CA1 neurons in slices in vitro. J. Neurosci. *29*, 12167–12173.

Saengsawang, W., Mitok, K., Viesselmann, C., Pietila, L., Lumbard, D.C., Corey, S.J., and Dent, E.W. (2012). The F-BAR protein CIP4 inhibits neurite formation by producing lamellipodial protrusions. Curr. Biol. *22*, 494–501.

Sasaki, J., Kofuji, S., Itoh, R., Momiyama, T., Takayama, K., Murakami, H., Chida, S., Tsuya, Y., Takasuga, S., Eguchi, S., et al. (2010). The PtdIns(3,4)P(2) phosphatase INPP4A is a suppressor of excitotoxic neuronal death. Nature *465*, 497–501.

Shimada, A., Niwa, H., Tsujita, K., Suetsugu, S., Nitta, K., Hanawa-Suetsugu, K., Akasaka, R., Nishino, Y., Toyama, M., Chen, L., et al. (2007). Curved EFC/F-BAR-domain dimers are joined end to end into a filament for membrane invagination in endocytosis. Cell *129*, 761–772.

Thewke, D.P., and Seeds, N.W. (1999). The expression of mRNAs for hepatocyte growth factor/scatter factor, its receptor c-met, and one of its activators tissue-type plasminogen activator show a systematic relationship in the developing and adult cerebral cortex and hippocampus. Brain Res. *821*, 356–367.

Tolias, K.F., Duman, J.G., and Um, K. (2011). Control of synapse development and plasticity by Rho GTPase regulatory proteins. Prog. Neurobiol. *94*, 133–148.

Tsujita, K., Suetsugu, S., Sasaki, N., Furutani, M., Oikawa, T., and Takenawa, T. (2006). Coordination between the actin cytoskeleton and membrane

deformation by a novel membrane tubulation domain of PCH proteins is involved in endocytosis. J. Cell Biol. *172*, 269–279.

Um, K., Niu, S., Duman, J.G., Cheng, J.X., Tu, Y.K., Schwechter, B., Liu, F., Hiles, L., Narayanan, A.S., Ash, R.T., et al. (2014). Dynamic control of excitatory synapse development by a Rac1 GEF/GAP regulatory complex. Dev. Cell *29*, 701–715.

Van Aelst, L., and D'Souza-Schorey, C. (1997). Rho GTPases and signaling networks. Genes Dev. *11*, 2295–2322.

Van de Ven, T.J., VanDongen, H.M., and VanDongen, A.M. (2005). The nonkinase phorbol ester receptor alpha 1-chimerin binds the NMDA receptor NR2A subunit and regulates dendritic spine density. J. Neurosci. *25*, 9488–9496.

Wang, X.B., Yang, Y., and Zhou, Q. (2007). Independent expression of synaptic and morphological plasticity associated with long-term depression. J. Neurosci. *27*, 12419–12429.

Xu, X., Miller, E.C., and Pozzo-Miller, L. (2014). Dendritic spine dysgenesis in Rett syndrome. Front. Neuroanat. *8*, 97.